Double impact dynamic test of a ground support system: An analysis through numerical methods

JA Vallejos Department of Mining Engineering and Advanced Mining Technology Center, University of Chile, Chile

M Fuentealba Advanced Mining Technology Center, University of Chile, Chile

E Marambio Advanced Mining Technology Center, University of Chile, Chile

L Burgos Advanced Mining Technology Center, University of Chile, Chile

R Brändle Geobrugg, Switzerland

R Luis Fonseca Geobrugg, Switzerland

G von Rickenbach Geobrugg, Switzerland

G Fischer Geobrugg, Switzerland

ABSTRACT

In underground excavations, under high stress conditions, ground support systems must provide safe and effective response to dynamic events. These systems must be capable to resist dynamic impacts and yielding during the loading process. In this context dynamic testing of the reinforcement and retaining elements that compose the ground support system are required to study and improve the behaviour of these elements under dynamic load events. During the last years, Geobrugg has been working on the improvement of retaining products by testing them in a large-scale impact test facility located at Walenstadt, Switzerland. The test facility is composed of a double level platform with a square-shaped pyramidal trunk geometry, in the upper level housing a loading mass that drop from a height up to 5m. The loading mass is guided by one central steel pipe, and the impact occurs in the sample to be tested located at the lower level in a slab with an area of 3.6m × 3.6m where the ground support system is installed. During the last years, this innovative facility has been used to test several configurations of ground support systems. The results of these tests have enabled to improve the understating of the behaviour of ground support systems under dynamic loads. In this manuscript, the back analysis through numerical methods (central difference and Newmark's method) of a ground support system tested with a double dynamic impact in 2019 is presented.

INTRODUCTION

Mining conditions are becoming increasingly difficult due to ore deposits are getting deeper, which has resulted in high-stress environments causing many challenges to continue resource exploitation. One of the main issues is related to the occurrence of seismic events and the associated rockburst phenomenon, that leads operational and safety problems.

The amount of energy release during seismic events requires to be mitigated by ground support systems (reinforcement plus retention systems) able to control large displacements and high strain rates. These dynamic systems are composed of reinforcement elements (e.g. rockbolts, cablebolts) able to absorb a large amount of energy and surface support (e.g. meshes) that provide containment to the rock mass (Zhou & Zhao, 2011).

The design of ground support systems requires research into the behaviour of each support element under dynamic loading. Previously, several tests have been carried out to individual bolts, cables, and meshes, but in the practice, all components must fit and work together. Thus, the testing is relevant to assess and increase, if necessary, the performance of support elements and offer to industry improved designs. Some institutions in Canada, South Africa and Australia have been testing reinforcement and support elements under dynamic loads. However, the facilities that can test the combinations (reinforcement or ground support systems) of rockbolts, cablebolts, and mesh as a system are limited.

Over the years, large-scale tests have been conducted in the rockfall testing facility at Walenstadt, Switzerland, that has contributed to improve the knowledge and try different types of test configurations and sample configurations (Brändle et al. 2017; Brändle & Luis Fonseca 2019; Bucher et al. 2013; Cala et al.

2013; Muñoz et al. 2017; Brändle et al., 2020; Roth et al., 2014). This paper presents a summary of a double impact dynamic test performed in 2019 and a back analysis through numerical methodologies (central difference and Newmark's method) for the ground support system tested.

DYNAMIC LABORATORY TESTS AND SUMMARY OF THE DOUBLE IMPACT TEST

During the last 30 years, significant effort has been made to obtain and quantify the dynamic response of a complete ground support system to provide solutions for rockburst control in high stress mining environments. Testing and measurements of dynamic response of isolated components that compose the ground support system, such as rockbolts, cablebolts or meshes, conducted by a number of institutions, including CanMet-MMSL, WASM and New Concept Mining (Crompton et al. 2018; Kaiser et al. 1996; Player et al. 2004). In addition, simplified retention (load distribution) and ground support systems have been tested by projects, such as SIMRAC/SRK or GRC (Cai & Kaiser 2018; Kaiser et al. 1996; Ortlepp 2001; Ortlepp & Stacey, 1998, 1997) using the impact principle and the momentum transfer concept (WASM). Table 1 illustrates a summary of the facilities that test configurations of ground support or retention (load distribution) systems.

Table 1. Summary of the facilities that test ground support or load distribution systems (Hadjigeorgiou & Potvin 2011)

Facility	Configuration /Element Tested	Loading Mass (kg)	Drop Height (m)	Impact velocity (m/s)	Impact energy (kJ)	Test area	Measurement instruments
WASM Dynamic facility	Reinforcement elements and surface support	Up to 4,500	Up to 6	Up to 10	Up to 225	1 m × 1 m	High-speed cameras, photographs, load cells, accelerometers and reference tapes
SRK Drop weight test	Support system	Up to 2,700	3.3	8.1	Up to 80	2 m × 2 m	High-speed cameras, photographs and reference tapes
SIMRAC Dynamic testing rig	Support system	1,000					Telescopic bars and geophones
SIMRAC Dynamic stope test	Stope support system	10,000	3	7.7	Up to 294	3 m × 3 m	High-speed cameras, photographs and reference tapes
GRC Support element test	Reinforced shotcrete	565	4	8.8	22		Load cells and photographs
Geobrugg Walenstandt test	Support system	Up to 9,640	5	10	Up to 500	3.6 m × 3.6 m	High-speed cameras, photographs, accelerometers, load cells and reference tapes

The dynamic testing of retaining and ground support systems have been limited due to the difficulty in represent the in-situ conditions of a seismic event, quantify the damage, measure and validate the response of each element and the interaction among them. Geobrugg has been performing real-scale dynamic tests on ground load distribution and ground support systems using the impact principle (drop weight test) since the research program started by Cala et al. (2013) through its facility at Walenstadt, Switzerland. The Walenstadt facility has been improved over the years in order to better represent and understand the damage process that occurs to a complete ground support system during a dynamic impact that represents the in-situ conditions

of a seismic event (Brändle et al. 2017; Brändle & Luis Fonseca 2019; Bucher et al. 2013; Cala et al. 2013; Muñoz et al. 2017; Brändle et al., 2020; Roth et al., 2014). Figure 1a and b show a schematic of the dynamic testing facility at Walenstadt used in the double impact test, whereas Figure 1c illustrates the current facility in-situ.

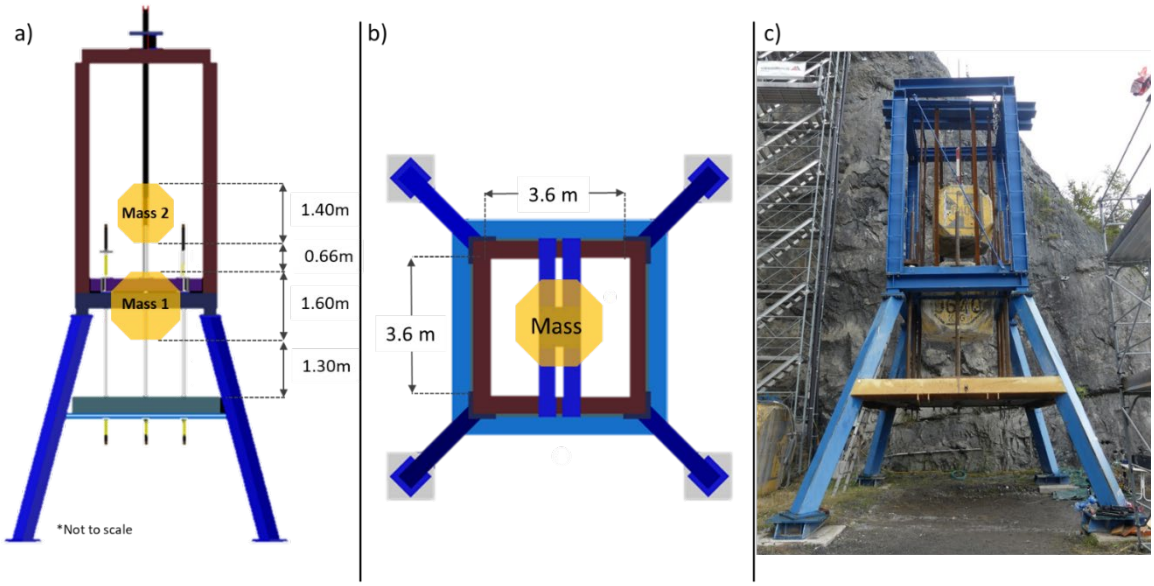

Figure 1. (a) Front view of testing setup, (b) plan view of testing setup, and (c) Dynamic test facility at Walenstadt

Test arrangement, ground support system, and measurement equipment

The testing setup to perform and record the double impact dynamic test comprised the following components:

- Steel pipes of 10mm thickness with an inner diameter of 45mm that represent the boreholes in which the rockbolts are installed in-situ. In this test 9 steel pipes were used (for varying rockbolt patterns), and the central steel pipe also served as a guide for the loading mass.
- A lower loading mass (mass 1 in Figure 1a) of 9,640kg released in a free fall condition along the central steel pipe from a height of 1.30m.
- An upper loading mass (mass 2 in Figure 1a) of 6,400kg released in a free fall condition along the central steel pipe from a height of 1.96m. This second mass was attached to the first mass with cables and was released together.

It is evident in this arrangement that no distribution elements were used to transmit the input energy to the load distribution system tested. In addition, the use of two masses in the dynamic test represent the dynamic loading condition of a typical seismic event where the tested ground support system is commonly used. In this sense, the length of the cables that join both masses represented the time gap between the two impacts proportional to the in-situ seismic event registered.

The test set up (sample) was built based on a similar ground support system used at CODELCO - El Teniente Mine, which includes:

- A load distribution system with a test area of 3.6 m × 3.6 m composed by a first layer of shotcrete with a thickness of 5 cm; a first Geobrugg's chain link mesh (internal) made of high-tensile steel wire with a diameter of 4 mm (MINAX 80/4); a second layer of shotcrete with a thickness of 2 cm; and a second Geobrugg's MINAX 80/4 mesh (external).
- A reinforcement system composed by nine threadbars (rockbolts) with a diameter of 25 mm, a length of 4 m and made of A630 Chilean steel grade. The rockbolts were located in a square pattern of 1 m × 1m and embedded into the steel pipes with cement grout. After curing each rockbolt was attached to the load

distribution system using a double plate and double nut (one pair per mesh). In this case, each rockbolt was debonded by sheathing covering a length of 50 cm from the collar (load distribution system) to represent the fractured rock zone in-situ. Figure 2 a and b illustrate the test configuration with each rockbolt identified (ID number) from an upper and lower view of the ground support system, respectively.

Note that the load distribution system is built before testing with enough time to cure the shotcrete at least 28 days and is subsequently attached to the load distribution system on the frame. Figure 3 shows a cross section scheme of the ground support system tested.

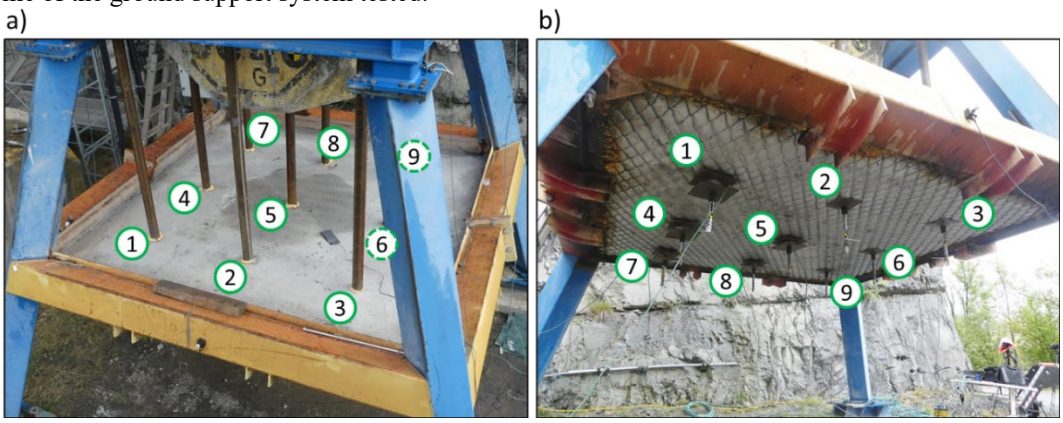

Figure 2. (a) Upper view, and (b) lower view of the test configuration with each rockbolt identified (ID number)

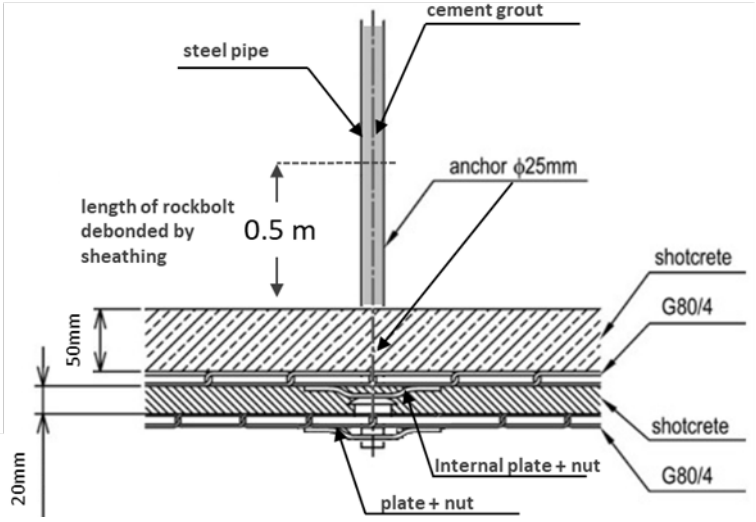

Figure 3. Cross section of the ground support system tested

The measurement system used for the test included:

- Four high-speed cameras with a recording frecuency of 500 images per second: a first camera pointing to the upper area (internal face) of the load distribution system, a second pointing to the lower area (external face) of the load distribution system, a third camera pointing to the upper area (external face) of the load distribution system located at 90 degrees from the first camera, and a fourth camera pointing to the lower area (external face) of the load distribution system located at 90 degrees from the second camera.
- Two accelerometers were located at the lateral edge of each loading mass. The accelerometers have a capacity of 2,000g with a frequency of 20kHz.

- Ten load cells with a capacity of 750kN and a frequency of 4.8kHz were used: five located at the collar (external plate) and five located at the anchor (upper part of the reinforcement system) of five rockbolts (i.e., rockbolts 1, 4, 5, 7 and 8 in Figure 2), with the assumption of symmetrical response of the rockbolts due to the pattern of the reinforcement system.
- Reference tapes located in each rockbolt and reference rulers to support the measurement of the high-speed cameras. The tapes have a square pattern of $1cm^2$ and the rulers have a pattern of 10cm.
- A coordinate reference system located in the middle of the load distribution system (origin) to support the measurement of the dynamic displacement. The positive axes point to the right (x), back (y) and upwards (z) (see Figure 3c).

TEST RESULTS

The behaviour of the ground support system was recorded and analysed using the information collected by the measurement system. The impact loading masses were arrested to an equilibrium state by the ground support system with a final dynamic displacement of 0.29 m, and an impacted area located at the center of the load distribution system as illustrated in Figure 4. The impact of the loading masses caused the failure of the rockbolt number 5 (central rockbolt) and some plates of other rockbolts caused the cut of the internal mesh. Figure 5 illustrates the dynamic process recorded by the high-speed cameras at different instants of time.

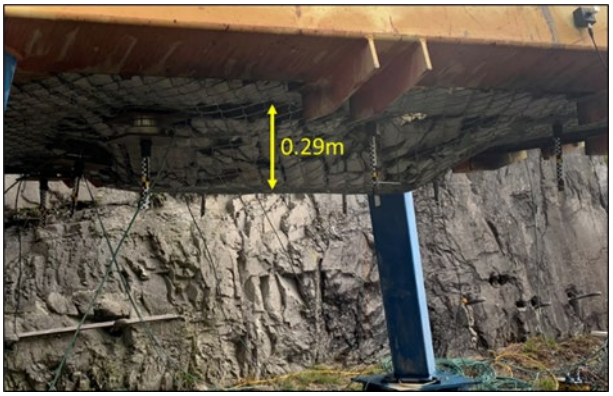

Figure 4. Final state of the ground support: Bagging area.

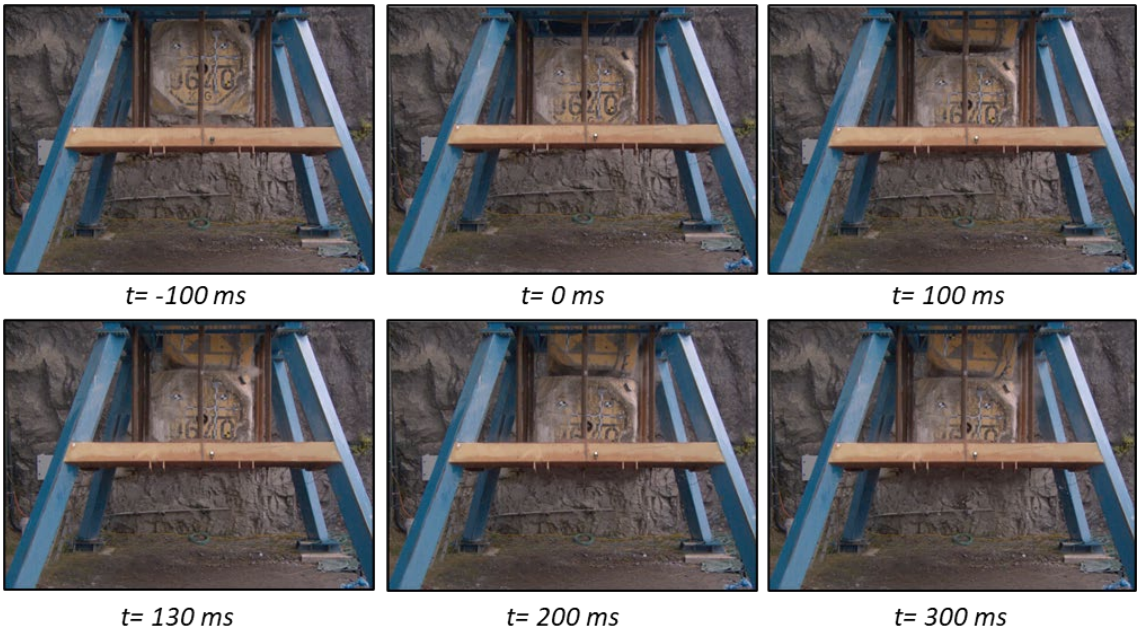

Figure 5. Dynamic loading process of the test recorded by the high-speed cameras as a function of time

ANALYSIS THROUGH NUMERICAL METHODS

Ground support systems are subjected to complex interactions during processes of dynamic loading. However, during the execution of dynamic tests the loads are controlled and then the displacement (deformation) of the system. Therefore, under controlled conditions is possible to simplify the system as concentrated masses supported by a structure without mass. In this new system, to represent the response of the real system, the minimum number of necessary coordinates to describe the deformation of the system defines its degrees of freedom (Rojas, 2018).

In structural dynamics, one of the simplest cases of analysis is the damped oscillator with a single degree of freedom, as shown in Figure 6. This system is composed of a concentrated mass supported by a spring (which represents the stiffness of the system) and a damping system that dissipates energy during the motion (restricted in a single direction).

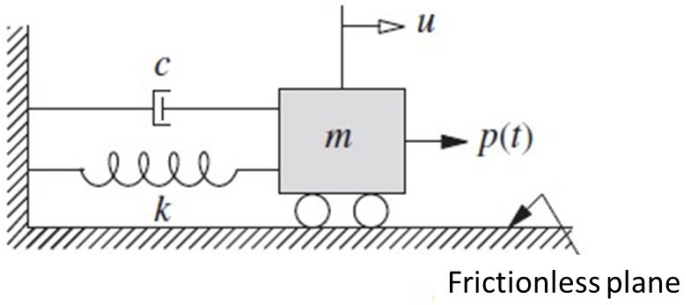

Figure 6. Damped oscillator with a single degree of freedom (Chopra, 2017).

When the system of the Figure 6 is subjected to a dynamic load, that depends on time, the mass will also move (displacement) though the time. Then, through the application of the second law of Newton is possible to determine the equation of motion of the system (Chopra, 2017).
A free body diagram is illustrated in Figure 7. Considering this diagram, the sum of forces can be represented in equation (1). Whereas the motion for a linear and a non-linear system can be represented through the equations (2) and (3), respectively. Where, m is the mass; k is the elastic stiffness; c is the viscous damping coefficient; $u(t)$ is the displacement over time; $\dot{u}(t)$ is the velocity over time; $\ddot{u}(t)$ is the acceleration over time; $fs(u)$ is the restoring force for a non-linear system (it depends on the displacement); and $F(t)$ is an external dynamic load.

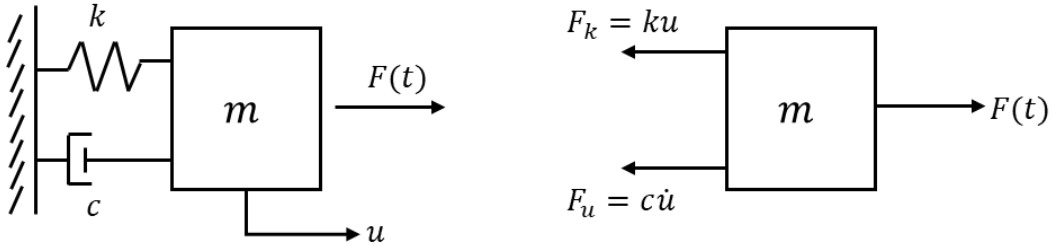

Figure 7. Free body diagram of a damped oscillator with a single degree of freedom (Rojas, 2018).

$$\sum F = m\ddot{u}(t) = -ku(t) - c\dot{u}(t) + F(t) \quad (1)$$

$$m\ddot{u}(t) + c\dot{u}(t) + ku(t) = F(t) \quad (2)$$

$$m\ddot{u}(t) + c\dot{u}(t) + fs(u) = F(t) \quad (3)$$

To determine the response of the system in Figure 6, it is necessary to solve its equation of motion, which depends on the external force that interacts with the system. For cases with no external forces, or with a harmonic force (periodic), or even with a constant force over time, there is an analytical solution to the

problem. However, in cases where the load cannot be represented by a mathematical expression, the numerical integration methods are useful to determine the response of dynamic systems.

It should be noted that several authors (Marambio et al., 2020, 2018; Morton et al., 2007; Nilsson, 2009; St-Pierre, 2007; Vallejos et al., 2020; among others) have worked previously with these simplified systems to represent reinforcement elements, retention elements, or the interaction between them (support systems) under dynamic loads. These models have improved the understanding of these elements and their internal behaviour when they are subjected to dynamic events.

Dynamic response through numerical integration methods

As stated above, in cases where the load cannot be represented by a mathematical expression, the numerical integration methods are useful to determine the response of dynamic systems, i.e., the equation of motion (Chopra, 2017; Rojas, 2018).
The fundamentals that define the numerical integration methods are listed below (Rojas, 2018):

1. The equation of motion is achieved only in discrete time intervals, i.e., in each Δt.
2. For any time t, the variation of displacement, velocity and acceleration between each time interval is assumed to be an established rule.

According to the methodology to determine the solution, the numerical integration methods can be divided into explicit and implicit methods (Rojas, 2018). The explicit methods are based on the information provided by the time i to calculate the solution at time $i+1$. Whereas the implicit methods calculate the solution at time $i+1$ based on the solution at time i, but considering the information at time $i+1$.

Based on the above, the method of central difference and the Newmark's method are described in detail (Chopra, 2017) below. These were used to describe the response of the ground support system in the dynamic double impact test.

Method of central difference

The central difference method is an explicit method based on the approximation of the velocity ($\dot{u}_i$) and acceleration ($\ddot{u}_i$) by finite differences. Considering a constant step of time ($\Delta t_i = \Delta t$), the approximations are illustrated in equation (4). Where, u_i represents the displacement at time i.

$$\dot{u}_i = \frac{u_{i+1} - u_{i-1}}{2\Delta t} \qquad \ddot{u}_i = \frac{u_{i+1} - 2u_i + u_{i-1}}{(\Delta t)^2} \tag{4}$$

The approximations in equation (4) are replaced in the equation of motion for linear (equation 2) or non-linear (equation 3) systems. Then, organizing the terms, the value u_{i+1} is described by equations (5), (6) and (7).

$$u_{i+1} = \frac{\hat{p}_i}{\hat{k}} \tag{5}$$

Where:

$$\hat{k} = \frac{m}{(\Delta t)^2} + \frac{c}{2\Delta t} \tag{6}$$

$$\hat{p}_i = p_i - \left[\frac{m}{(\Delta t)^2} - \frac{c}{2\Delta t}\right] u_{i-1} + \frac{2m}{(\Delta t)^2} u_i - (f_S)_i \tag{7}$$

Note that equation (7) appears to be described for a non-linear system. However, it is easily extrapolated to a linear system by replacing the last term (right) with ku_i (elastic force).

Therefore, the algorithm to solve the problem trough the method of central difference is presented below:

1. Initial calculation

    1.1. Determine k, c y m
    1.2. Calculate the initial acceleration $\ddot{u_0} = \frac{p_0 - c\dot{u_0} - (f_S)_0}{m}$
    1.3. Select an appropriated Δt
    1.4. Calculate $\hat{k}$ according to equation (6)

2. Calculation at each time step i

    2.1. Calculate $\hat{p}_i$ according to equation (7)
    2.2. Calculate u_{i+1} according to equation (5)
    2.3. Calculate $\dot{u}_i$ y $\ddot{u}_i$ according to equation (4)

3. Repeat at the next time step $(i + 1)$

    3.1. Repeat the steps 2.1, 2.2 y 2.3 at time step $i + 1$.

Newmark's method

Newmark developed a family of methods in time step by step based mainly on the equations (8) and (9). Where, the parameters β and γ define the variation of acceleration during a time interval, and the stability and precision of the method. Typically, the selection for these parameters is $\gamma = \frac{1}{2}$ and $\frac{1}{6} \leq \beta \leq \frac{1}{4}$.

$$\dot{u}_{i+1} = \dot{u}_i + [(1-\gamma)\Delta t]\ddot{u}_{i+1} \tag{8}$$

$$u_{i+1} = u_i + (\Delta t)\dot{u}_i + [(0.5-\beta)\Delta t]\ddot{u}_i + [\beta(\Delta t)^2]\ddot{u}_{i+1} \tag{9}$$

The Newmark's method is implicit, then determines the solution at time $i + 1$ from the equilibrium condition at time $i + 1$. From u_i, $\dot{u}_i$ and $\ddot{u}_i$ values known at time i, the values u_{i+1}, $\dot{u}_{i+1}$ y $\ddot{u}_{i+1}$ are calculated combining the equations (8) and (9) with the motion equation of the system (linear or non-linear). The equation (9) can be organized in terms of u_{i+1}, resulting in equation (10).

$$\ddot{u}_{i+1} = \frac{1}{\beta(\Delta t)^2}(u_{i+1} - u_i) - \frac{1}{\beta \Delta t}\dot{u}_i - \left(\frac{1}{2\beta} - 1\right)\ddot{u}_i \tag{10}$$

Then replacing equation (10) in equation (8), equation (11) is obtained.

$$\dot{u}_{i+1} = \frac{\gamma}{\beta \Delta t}(u_{i+1} - u_i) + \left(1 - \frac{\gamma}{\beta}\right)\dot{u}_i + \Delta t\left(1 - \frac{\gamma}{2\beta}\right)\ddot{u}_i \tag{11}$$

Considering a non-linear system, the equation of motion at time $i + 1$ is represented by equation (12).

$$m\ddot{u}_{i+1} + c\dot{u}_{i+1} + (f_S)_{i+1} = F_{i+1} \tag{12}$$

The restoring force $(f_S)_{i+1}$ for a non-linear system is an implicit function of the unknown value u_{i+1}, then an iteration is required. Therefore, the equation (12) can be expressed in a new form where the restoring force includes the terms of inertia and damping, resulting in equation (13) (detailed in equation (14)).

$$\widehat{(f_S)}_{i+1} = F_{i+1} \tag{13}$$

$$\widehat{(f_S)}_{i+1} = m\ddot{u}_{i+1} + c\dot{u}_{i+1} + (f_S)_{i+1} \tag{14}$$

This new definition allows to apply the Taylor series for equation (13) due to $\widehat{(f_S)}_{i+1}$ is interpreted as function of the displacement u_{i+1}. After neglecting the second order and higher terms, obtaining the derivative of equation (14), and determining the inertia and damping terms from equations (8) and (9), the tangent stiffness $\widehat{(k_T)}_{i+1}^{(j)}$ for iteration j is defined as shown in equation (15).

$$\widehat{(k_T)}_{i+1}^{(j)} = \frac{1}{\beta(\Delta t)^2}m + \frac{\gamma}{\beta\Delta t}c + (k_T)_{i+1}^{(j)} \tag{15}$$

Using this definition, the equation (16) can be obtained (detailed in equation (17)). Where $\hat{R}_{i+1}^{(j)}$ represents a residual force for iteration j.

$$\widehat{(k_T)}_{i+1}^{(j)}\Delta u^{(j)} = F_{i+1} - \left(\hat{f}_S\right)_{i+1}^{(j)} \equiv \hat{R}_{i+1}^{(j)} \tag{16}$$

$$\Delta u^{(j)} = u_{i+1}^{(j+1)} - u_{i+1}^{(j)} \tag{17}$$

Replacing equation (10) and (11) in equation (14) and combining the result with the right side of equation (16), an expression for the residual force can be obtained as illustrated in equation (18).

$$\begin{aligned}\hat{R}_{i+1}^{(j)} = F_{i+1} - (f_S)_{i+1}^{(j)} - \left[\frac{1}{\beta(\Delta t)^2}m + \frac{\gamma}{\beta\Delta t}c\right]\left(u_{i+1}^{(j)} - u_i\right) + \left[\frac{1}{\beta\Delta t}m + \left(\frac{\gamma}{\beta} - 1\right)c\right]\dot{u}_i \\ + \left[\left(\frac{1}{2\beta} - 1\right)m + \Delta t(\frac{\gamma}{2\beta} - 1)c\right]\ddot{u}_i\end{aligned} \tag{18}$$

From the expressions presented above, the algorithm to solve the Newmark's method is introduced:

1. Initial calculation
    - 1.1. Determine the initial state: $(f_S)_0$ and $(k_T)_0$
    - 1.2. Calculate $\ddot{u_0} = \frac{p_0 - c\dot{u}_0 - (f_S)_0}{m}$
    - 1.3. Select an appropriated Δt
2. Calculate for time steps $i = 0, 1, 2, 3, ...$
    - 2.1. Initialize for $j = 1$, $u_{i+1}^{(j)} = u_i$, $(f_S)_{i+1}^{(j)} = (f_S)_i$, and $(k_T)_{i+1}^{(j)} = (k_T)_i$
3. For each iteration $j = 1, 2, 3, ...$
    - 3.1. Calculate $\hat{R}_{i+1}^{(j)}$ according to equation (18)
    - 3.2. Verify the convergence. If convergence is achieved go to step 4., else continue to the next step.
    - 3.3. Calculate $\widehat{(k_T)}_{i+1}^{(j)}$ according to equation (15)
    - 3.4. Calculate $\Delta u^{(j)}$ according to equation (16)
    - 3.5. Calculate $u_{i+1}^{(j+1)}$ according to equation (17)
    - 3.6. Determine the state: $(f_S)_{i+1}^{(j+1)}$ and $(k_T)_{i+1}^{(j+1)}$
    - 3.7. Replace j with $j + 1$ and repeat steps 3.1 to 3.6. Specify the final value of u_{i+1}
4. Calculation of velocity and acceleration
    - 4.1. Calculate $\dot{u}_{i+1}$ according to equation (11)
    - 4.2. Calculate $\ddot{u}_{i+1}$ according to equation (10)
5. Repetition for the next time step
    - 5.1. Repeat the steps 2. to 4. for time step $i + 1$

IMPLEMENTATION OF THE NUMERICAL METHODS AND RESULTS

Implementation and input for numerical methods

To determine the numerical dynamic response in terms of displacement and load of the ground support system tested, the equation of motion (equation (2)) was solved through the numerical methods of central difference and Newmark.

Using the algorithms previously presented, both methods of numerical integration were implemented in a program built in Python. As a part of the resolution, the dynamic increase factor (DIF) introduced by Malvar and Crawford (1998) was considered. To validate the program (and the numerical methods), a dynamic test result from WASM (Player et al., 2004) with known parameters was modeled with satisfactory results. Note that this result was used only to verify the performance of the central rockbolt (threadbar) under laboratory-scale conditions. A similar validation was used previously by Marambio et al. (2018) and Vallejos et al. (2020).

Once the numerical methods were validated, the numerical dynamic response of the ground support system tested was determined. To achieve this response, the numerical methods were implemented considering the input parameters of the dynamic test and the ground support system tested as shown in Table 2.

Table 2. Input parameters of the numerical methods

Mass of the oscillator, $m\ [kg]$	410
Viscous damping coefficient, $c\ [Ns/mm]$	195
Equivalent stiffness, $k\ [kN/mm]$	19.4
Initial position, $u_0\ [m]$	0
Initial velocity, $v_0\ [m/s]$	0
Yielding point of reinforcement, $f_y[MPa]$	420
Time step, $\Delta t\ [s]$	0.002
Time of analysis, $t_f\ [s]$	0.3

Note that the mass of the oscillator is considered as the sum of the elements that compose the area of ground support system affected by the test (2.56 m^2). The stiffness of the oscillator is an equivalent stiffness representing the sum of the reinforcement stiffness and retention stiffness. Whereas the viscous damping coefficient was determined through an iterative process, adjusting the numerical response with the real response. In this case, the external force is given by the acceleration record of the lower block (Figure 1a) in the test.

To implement the DIF (Malvar and Crawford, 1998) to the reinforcement elements, the yielding point of the steel (according to its steel grade) was considered. In addition, due to the loading masses in free fall impact the ground support system, the initial position of the oscillator is zero. Finally, to determine the numerical dynamic response of the ground support system, the time of analysis is the same time recorded for the test.

Thus, is possible to implement the numerical methods previously illustrated to reproduce the response in terms of load–displacement. Additionally, with the components of damping and yielding point is possible to obtain the dissipated energy as function of time and displacement.

Numerical response of the ground support system tested

The numerical response of the ground support system tested (double impact) was obtained using the numerical methods previously illustrated and the input parameters shown in Table 2.

Figure 8 shows the numerical response of the ground support system in terms of displacement as a function of time. In this graph, the real response of the ground support system (measured) is compared with the response of the numerical methods (central difference and Newmark). Similarly, Figure 9 illustrates the load-displacement response of the central rockbolt. Here, the real response (measured) of the central rockbolt is compared with the numerical response obtained by the numerical methods.

In addition, the dissipated energy of the ground support system is shown in Figure 10. In this graph, the real response is compared with the numerical response obtained by the numerical methods. Note that the dissipated energy is estimated as the sum of the integration of the load-displacement response for each element that compose the ground support system (Chopra, 2017).

Finally, it should be noticed that the performance of the central rockbolt (Figure 9) is well described by the algorithms. Whereas the behaviour of the ground support system (Figure 8 and Figure 10) under the test has a good correlation with the response from algorithms, despite the difference in the final displacement and dissipated energy.
This difference in response can be associated with the simplicity of the model considered for the ground support system (damped oscillator) and the parameters used. In the case of the central rockbolt, the response of the model is more precise due to the previous validation and the consideration of parameters previously described by other authors (Marambio et al., 2018; St-Pierre, 2007; Vallejos et al., 2020; among others).

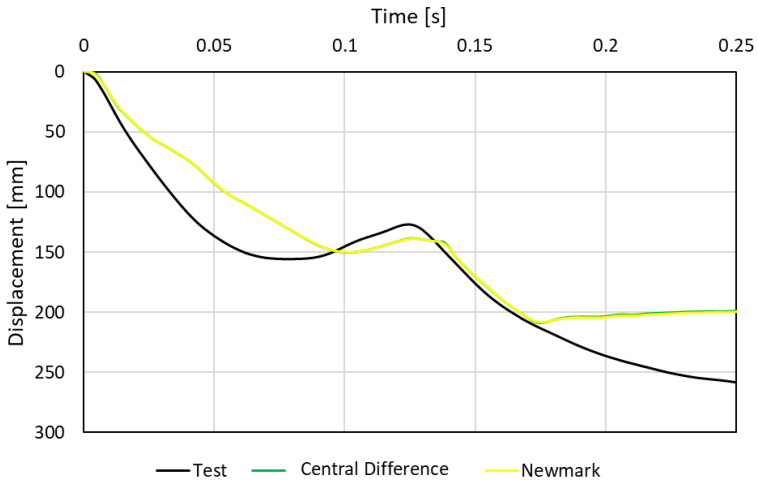

Figure 8. Numerical and real response of the ground support system for the displacement

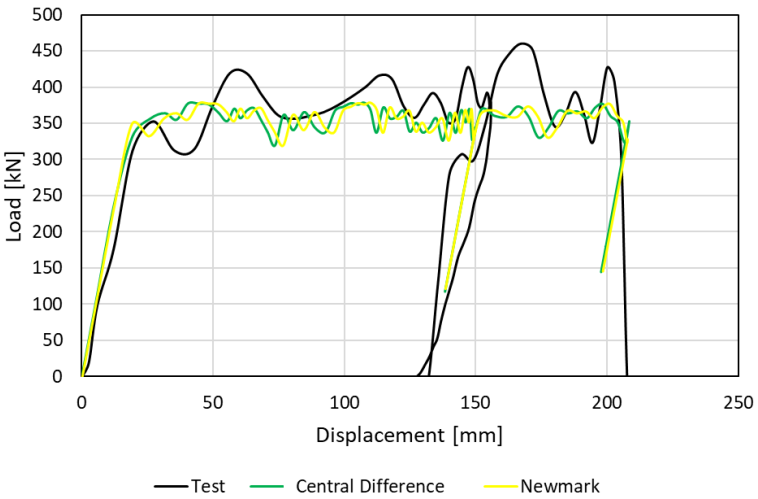

Figure 9. Numerical and real response of the central rockbolt in terms of load and displacement

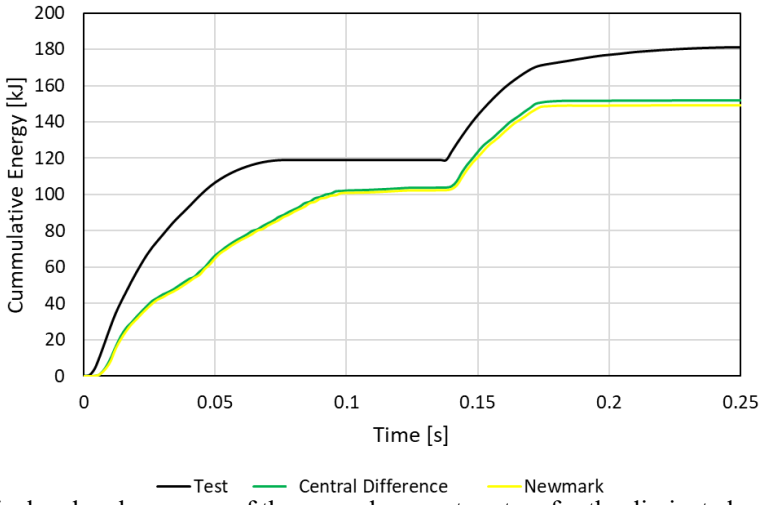

Figure 10. Numerical and real response of the ground support system for the dissipated energy over time

CONCLUSIONS

Laboratory-scale dynamic tests contribute to the knowledge, standardization, and certification of different configurations of ground support systems. The test arrangement on this occasion allowed to study under laboratory-scale conditions the damage process in a recreated seismic event (rockburst condition) where the ground support system is commonly used.

The numerical methods (central difference and Newmark) were validated (previously) and implemented satisfactorily. They have a good correlation with the load-displacement response (measured) of the ground support system and especially with the central rockbolt, reproducing their elastic and plastic responses.

Both methods have no major differences between them possibly due to the time step used. Then both methods converged to a satisfactory solution.

In the case of the yielding point, the use of DIF (Malvar and Crawford, 1998) agrees with the real response (measured) of the central rockbolt, giving a good approximation of the real behaviour as was shown previously by Marambio et al. (2018) and Vallejos et al. (2020).

The numerical methods underestimate the displacement and then the dissipated energy of the ground support system. The response possibly was influenced by the input parameters of the methods and the use of a simple model (damped oscillator with a single degree of freedom) to represent the problem. However, the central difference method and the Newmark's method represent a quick tool to estimate the response of the ground support system (and the reinforcement elements) under dynamic load conditions.

Despite the results, these well-calibrated numerical tools can rapidly complement and improve the understanding of laboratory-scale tests for ground support systems under dynamic conditions. This is a positive aspect considering the preparation time and costs associated with each dynamic test.

ACKNOWLEDGEMENT

The authors sincerely acknowledge the support from Geobrugg to collaborate with the dynamic testing facility at Walenstadt to perform the test and actively participate during the analysis and elaboration of this document. Finally, the authors acknowledge the support from the basal CONICYT Project AFB180004 of the Advanced Mining Technology Center (AMTC) – University of Chile.

The opinions expressed in this paper are those of the authors and do not necessarily represent the views of any other individual or organization.

REFERENCES

Brändle, R., Luis Fonseca, R., 2019. Dynamic testing of surface support systems. Ninth Int. Symp. Gr. Support Min. Undergr. Constr.

Brändle, R., Luis Fonseca, R., von Rickenbach, G., Fischer, G., Vallejos, J., Marambio, E., Burgos, L., Rojas, E., Landeros, P., Muñoz, A., Celis, S., Castro, D., 2020. Double impact dynamic test of a ground support system at the Walenstadt testing facility. MassMin 2020 Eighth Int. Conf. Exhib. Mass Min.

Brändle, R., Rorem, E., Luis Fonseca, R., Fischer, G., 2017. Full-scale dynamic tests of a ground support system using high-tensile strength chain-link mesh in El Teniente mine, Chile, in: Proceedings of the First International Conference on Underground Mining Technology. Australian Centre for Geomechanics, pp. 25–43.

Bucher, R., Cala, M., Zimmermann, A., Balg, C., Roth, A., 2013. Large scale field tests of high-tensile steel wire mesh in combination with dynamic rockbolts subjected to rockburst loading. Seventh Int. Symp. Gr. Support Min. Undergr. Constr.

Cai, M., Kaiser, P.K., 2018. Rockburst Support Reference Book. Volume I: Rockburst phenomenon and support characteristics. MIRARCO - Min. Innov. Laurentian Univ. Sudbury, Ontario, Canada.

Cala, M., Roth, A., Roduner, A., 2013. Large scale field tests of rock bolts and high-tensile steel wire mesh subjected to dynamic loading, in: ISRM International Symposium-EUROCK 2013. International Society for Rock Mechanics and Rock Engineering.

Chopra, A.K., 2017. Dynamics of structures. theory and applications to. Earthq. Eng.

Crompton, B., Berghorst, A., Knox, G., 2018. A new dynamic test facility for support tendons. New Concept Mining.

Hadjigeorgiou, J., Potvin, Y., 2011. A critical assessment of dynamic rock reinforcement and support testing facilities. Rock Mech. rock Eng. 44, 565–578.

Kaiser, P.K., McCreath, D.R., Tannant, D.D., 1996. Canadian rockburst support handbook. Geomech. Res. Centre, Laurentian Univ. Sudbury 314.

Malvar, L.J., Crawford, J.E., 1998. Dynamic increase factors for steel reinforcing bars [C], in: 28th DDESB Seminar. Orlando, USA.

Marambio, E., Vallejos, J., Burgos, L., von Rickenbach, G., Fischer, G., Brändle, R., 2020. Numerical modelling of dynamic testing for surface retaining elements used in underground mining: Calibration. MassMin 2020 Eighth Int. Conf. Exhib. Mass Min.

Marambio, E., Vallejos, J.A., Burgos, L., Gonzalez, C., Castro, L., Saure, J.P., Urzua, J., 2018. Numerical modelling of dynamic testing for rock reinforcement used in underground excavations. Fourth Int. Symp. Block Sublevel Caving.

Morton, E.C., Thompson, A.G., Villaescusa, E., Roth, A., 2007. Testing and analysis of steel wire mesh for mining applications of rock surface support, in: 11th ISRM Congress. International Society for Rock Mechanics and Rock Engineering.

Muñoz, A., Brändle, R., Luis Fonseca, R., Fischer, G., 2017. Full-scale dynamic tests of a ground support system using high-tensile strength chain-link mesh in El Teniente mine. Proc. RaSiM9, Santiago, Chile.

Nilsson, C., 2009. Modelling of dynamically loaded shotcrete. Master Thesis, Royal Institute of Technology.

Ortlepp, W.D., 2001. Performance testing of dynamic stope support test facility at Savuka. SIMRAC Rep. GAP 611.

Ortlepp, W.D., Stacey, T.R., 1998. Performance of tunnel support under large deformation static and dynamic loading. Tunn. Undergr. Sp. Technol. 13, 15–21.

Ortlepp, W.D., Stacey, T.R., 1997. Testing of tunnel support: dynamic load testing of rock support containment systems. SIMRAC GAP Proj. 221, 1997.

Player, J.R., Villaescusa, E., Thompson, A.G., 2004. Dynamic testing of rock reinforcement using the momentum transfer concept, in: Proceeding in 5th International Symposium on Ground Support, Villaescusa and Potvin (Eds), Perth, Balkema.

Rojas, F., 2018. Lecture of Structural Dynamics. Civil Engineering, University of Chile.

Roth, A., Cala, M., Brändle, R., Rorem, E., 2014. Analysis and numerical modelling of dynamic ground support based on instrumented full-scale tests, in: Proceedings of the Seventh International Conference on Deep and High Stress Mining. Australian Centre for Geomechanics, pp. 151–163.

St-Pierre, L., 2007. Development and validation of a dynamic model for a cone bolt anchoring system. M.Eng. thesis, McGill University.

Vallejos, J.A., Marambio, E., Burgos, L., Gonzalez, C. V, 2020. Numerical modelling of the dynamic response of threadbar under laboratory-scale conditions. Tunn. Undergr. Sp. Technol. 100, 103263.

Zhou, Y., Zhao, J., 2011. Advances in rock dynamics and applications. CRC Press.